MEAN FLOW AND TURBULENT STATISTICS OF THE FLOW OVER A SUBMERGED SHARP-CRESTED WEIR.

Chaewoong Ban, Ph.D Candidate, Department of Civil & Environmental engineering, Yonsei University, Seoul, Korea
Sung-Uk Choi Professor, Department of Civil & Environmental engineering, Yonsei University, Seoul, Korea

1. Introduction

- Flow over a sharp-crested weir shows the free flow, where the critical flow occurs at the tip of the weir. However, as the discharge increases, the downstream water level affects the overflow and the flow over the weir becomes the submerged flow
- Wu and Rajaratnam (1996) divided the submerged flow into impinging jet and surface flow regimes. Surface flow regimes can further be classified into the surface jump (or breaking wave), surface wave, and surface jet.

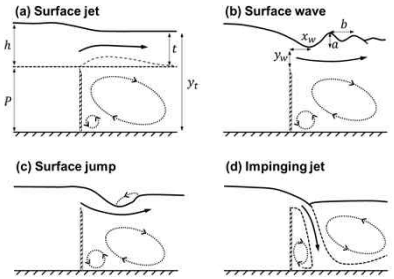

Figure 1. Classification of submerged flow regimes.

- Wu and Rajaratnam (1996) proposed a criterion to distinguish the impinging jet and the surface flow. The following relationships present the transition region from impinging jet to surface flow:

$$t/h = 1 - 0.215\lambda + 0.0142\lambda^2 - 0.00031\lambda^3 \quad \text{(for lower curve)}$$

$$t/h = 1 - 0.126\lambda + 0.0076\lambda^2 - 0.00017\lambda^3 \quad \text{(for upper curve)}$$

$\lambda = \sqrt{g(h-t)/(q/y_t)}$, g = gravity, h = head above the crest of the weir, t = depth of tailwater above the weir crest, q = unit discharge, y_t = tailwater depth

- which are the lower and upper bounds of the transition, respectively. The region between the upper curve and lower curve indicates the transition stage, where the flow regime is affected by the history of the flow, so-called the hysteresis effect.
- Azimi et al. (2016) also presented classification of submerged flows for $0.146 < h/P < 0.389$ based on t/h, where P = weir height. That is, impinging jet, surface jump, surface wave, and surface jet occur in the respective ranges of $t/h < 0.2$, $0.2 < t/h < 0.48$, $0.48 < t/h < 0.78$, and $t/h < 0.78$. The boundary between the surface wave and surface jet is defined when the amplitude of the wave becomes less than 10% of the approach flow head.

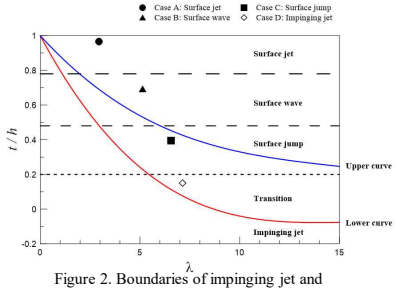

Figure 2. Boundaries of impinging jet and surface flow regimes.

- This research aims to study the flow characteristics of submerged flows over sharp-crested weirs in various flow regimes. The flows downstream of the weir are featured by highly 3D unsteady nature shed from the weir, requiring highly-resolved large eddy simulation (LES) to demonstrate the detailed flow structures. This study presents results of the LES of four different flow regimes to investigate the mean flow and turbulent structures.

2. GOVERNING EQUATIONS

- Filtered Navier-Stokes equations

$$\frac{\partial \overline{u_i}}{\partial x_i} = 0$$

$$\rho\frac{\partial \overline{u_i}}{\partial t} + \rho\overline{u_j}\frac{\partial \overline{u_i}}{\partial x_j} = -\frac{\partial \overline{p}}{\partial x_i} + \frac{\partial}{\partial x_j}\left(\overline{\tau_{ij}} + \tau_{ij}^{sgs}\right) + \rho g_i$$

- Subgird (SGS) stress tensor

$$\tau_{ij}^{sgs} = \rho\left(\overline{u_i u_j} - \overline{u_i}\,\overline{u_j}\right) = 2\rho\nu_t\overline{S_{ii}} + \frac{1}{3}\delta_{ij}\tau_{kk}^{sgs}$$

- The SGS stress tensor is modeled by the wall-adapting local eddy viscosity (WALE) model, proposed by Nicoud & Ducros (1999).

3. Numerical framework

- The computations, three computational grids were used, namely coarse, intermediate, and fine grids for the surface jet case, and fine grids for the other cases. For the fine grid resolution, the maximum grid spacing is $\Delta = 5 \times 10^{-3}$ m. In the near-wall region, the grid size is $\Delta = 2.5 \times 10^{-3}$ m with a spatial average of $\Delta^+ \cong 13$. The number of grid cells is about 10.8×10^6 for the fine grid.

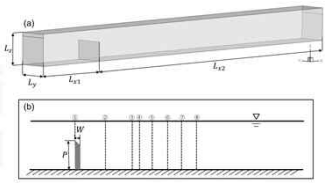

Figure 3. Computational domains: (a) 3D view; (b) side view.

- The inflow condition comes from a preliminary LES computation in a periodic channel of an identical cross-section. The velocity fields did not include fluctuations, but time-averaged velocity fields were fed into the inflow.
- For the free surface tracking, volume of fluid (VOF) method is used. Interface corresponding $\alpha = 0.5$ is considered as free surface.
- Hydraulic conditions for the surface jet are from the experiments by Rajaratnam and Muralidhar (1969). We made up the other three flow regimes satisfying the threshold proposed by both Wu and Rajaratnam (1996) and Azimi et al. (2016).

Table 1. Hydraulic conditions.

Case	Flow regime	B (m)	P (m)	h (m)	t (m)	Δh (m)	t/h	λ	q (m²/s)	U_b (m/s)	Fr	Re
A	Surface jet	0.457	0.302	0.141	0.136	0.005	0.965	2.955	0.033	0.0741	0.061	11,170
B	Surface wave	0.457	0.302	0.075	0.052	0.023	0.693	5.142	0.033	0.0867	0.073	12,340
C	Surface jump	0.457	0.302	0.071	0.028	0.043	0.394	6.554	0.033	0.0877	0.074	12,422
D	Impinging jet	0.457	0.302	0.067	0.010	0.057	0.149	7.135	0.033	0.0886	0.075	12,505

4. Results

- The velocity profiles show that the flow accelerates by passing over the weir and the backward flows occur near the bed.
- The overall agreement between the simulated velocity profiles and measured data is good.
- Three different grid resolutions are tested and Figure 4 confirms that the fine-mesh grid is accurate enough to converge the solution.

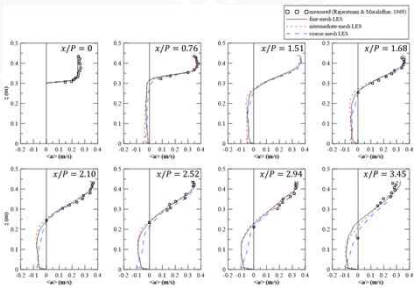

Figure 4. Time-averaged streamwise velocity profiles along the streamwise direction.

- Figures 5(a) and 5(b) show the toe of jump and trough of surface wave and Figure 5(c) and 5(d) show the dimensions of the first wave. In the figure, vertical line means the boundary of threshold between the flow regimes.
- Positions of the toe of jump and trough of surface wave are well predicted by the LES.

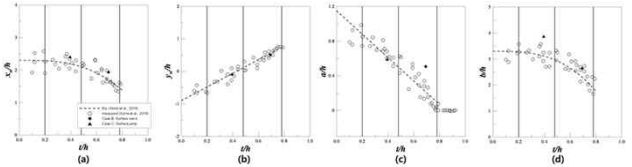

Figure 5. Position of the toe of jump/trough of surface wave (x_w/h, y_w/h) and dimensions of the first wave (a/h, b/h).

- Figure 6 present contours of time-averaged streamwise velocity with streamlines for the four different flow regimes. The LES results show that the four flow regimes show distinctive characteristics of the recirculation zones downstream of the weir and the free surface.
- Figure 6(a), a jet is made at the tip of the weir, forming a large primary vortex with a small weak vortex at the lower corner of the re-circulation zone. The contour plot indicates that reattachment takes place at $x/P = 7.6$.
- As t/h decreases, the surface wave is generated as can be seen in Figure 6(b). The jet flow becomes more intensive with the flow depth reduced over the tip of the weir. This resulted in stronger backward flows, increasing the size of the weak vortex at the lower corner.
- Figure 6(c) shows the surface jump, which is made as t/h decreases from the surface wave. The generation of the surface jump is confirmed by the presence of the surface vortex. Strong backward flows are observed in the vicinity of the bed.
- If t/h further decreases, then the impinging jet is generated. The overflow is heading the bed, with counter-rotating vortices formed about the overflow. The size of the weak vortex at the lower corner is observed to be larger than that of the weak vortices made in the other three flow regimes.

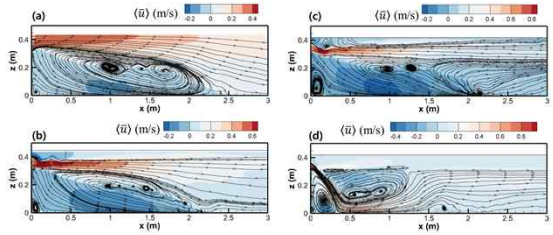

Figure 6. Contours of time-averaged streamwise velocity with streamlines: (a) Case A; (b) Case B; (c) Case C; (d) Case D.

5. Conclusions

- Large eddy simulation was carried out for turbulent flows over a submerged weir. Four different overflows, namely surface jet, surface wave, surface jump, and impinging jet, were simulated.
- The LES results were compared with the measured data by Rajaratnam & Muralidhar (1969), showing good agreement.
- Distinctive characteristics of the recirculation zones and the free surface were found and discussed.

References

- Azimi, A. H., Rajaratnam, N., and Zhu, D. Z. (2016). Water surface characteristics of submerged rectangular sharp-crested weirs. *Journal of Hydraulic Engineering*, 142(5), 06016001.
- Nicoud, F., and Ducros, F. (1999). Subgrid-scale stress modelling based on the square of the velocity gradient tensor. *Flow, Turbulence and Combustion*, 62(3), 183-200.
- Rajaratnam, N., and Muralidhar, D. (1969). Flow below deeply submerged rectangular weirs. *Journal of Hydraulic Research*, 7(3), 355-374.
- Wu, S., and Rajaratnam, N. (1996). Submerged flow regimes of rectangular sharp-crested weirs. *Journal of Hydraulic Engineering*, 122(7), 412-414.